Dynamical Aspects of Denatured Morris-Lecar Neurons

Indra Ghosh (https://indrag49.github.io)

School of Mathematical and Computational Sciences,
Massey University, New Zealand

April 25, 2025

Collaborators

(a) Hammed O. Fatoyinbo

(b) Sishu S. Muni

A brief survey of computational neuron dynamics models

- In 1952 Alan Hodgekin and Andrew Huxley developed a conductance-based model of how action potentials in neurons are propagated.

[1]NINDS. "Brain Basics: The Life and Death of a Neuron." (2019)

A brief survey of computational neuron dynamics models

- In 1952 Alan Hodgekin and Andrew Huxley developed a conductance-based model of how action potentials in neurons are propagated.
- This is mathematically modeled using a continuous-time dynamical system (ODEs), characterising the properties of excitable cells like neurons.

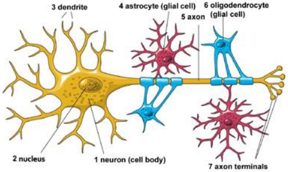

Figure: Schematic of a functional neuron[1].

[1] NINDS. "Brain Basics: The Life and Death of a Neuron." (2019)

A brief survey of computational neuron dynamics models

- Specifically, their model explains the time dynamics of action potential propagation in the *squid giant axon* from experiments.

Figure: Squid giant axon[2].

[2]Wikipedia (2019)

A brief survey of computational neuron dynamics models

- The Hodgekin-Huxley model uses four state-variables, namely the membrane potential (V), and the three uncoupled variables (functions of voltage and time) n, m, and h for the gated ion (sodium and potassium) channels.

Figure: Hodgekin and Huxley.

[3] Schwiening, Christof J. "A brief historical perspective: Hodgkin and Huxley". J. Physiol. 590.Pt 11 (2012): 2571–2575.

A brief survey of computational neuron dynamics models

- The Hodgekin-Huxley model uses four state-variables, namely the membrane potential (V), and the three uncoupled variables (functions of voltage and time) n, m, and h for the gated ion (sodium and potassium) channels.

Figure: Hodgekin and Huxley.

- Hodgekin and Huxley received the 1963 Nobel Prize in Physiology or Medicine for this work[3].

[3] Schwiening, Christof J. "A brief historical perspective: Hodgkin and Huxley". J. Physiol. 590.Pt 11 (2012): 2571–2575.

A brief survey of computational neuron dynamics models

- Since then, a notable number of neurodynamics models have been proposed.

[4] Morris, C. and Lecar, H. "Voltage oscillations in the barnacle giant muscle fiber". Biophys. J., 35, 193 (1981).

A brief survey of computational neuron dynamics models

- Since then, a notable number of neurodynamics models have been proposed.
- Popular ones include the *FitzHugh-Nagumo* model, the *Morris-Lecar* model, and the *Hindmarsh-Rose* model.

[4] Morris, C. and Lecar, H. "Voltage oscillations in the barnacle giant muscle fiber". Biophys. J., 35, 193 (1981).

A brief survey of computational neuron dynamics models

- Since then, a notable number of neurodynamics models have been proposed.
- Popular ones include the *FitzHugh-Nagumo* model, the *Morris-Lecar* model, and the *Hindmarsh-Rose* model.
- These models were driven by the need of reducing the complexity of the Hodgkin-Huxley model, which would essentially still replicate the dynamics.

---

[4] Morris, C. and Lecar, H. "Voltage oscillations in the barnacle giant muscle fiber". Biophys. J., 35, 193 (1981).

A brief survey of computational neuron dynamics models

- Since then, a notable number of neurodynamics models have been proposed.
- Popular ones include the *FitzHugh-Nagumo* model, the *Morris-Lecar* model, and the *Hindmarsh-Rose* model.
- These models were driven by the need of reducing the complexity of the Hodgkin-Huxley model, which would essentially still replicate the dynamics.
- Catherine Morris and Harold Lecar[4] proposed a two-dimensional "reduced" conductance-based description of the neuron dynamics.

[4] Morris, C. and Lecar, H. "Voltage oscillations in the barnacle giant muscle fiber". Biophys. J., 35, 193 (1981).

A brief survey of computational neuron dynamics models

- Since then, a notable number of neurodynamics models have been proposed.
- Popular ones include the *FitzHugh-Nagumo* model, the *Morris-Lecar* model, and the *Hindmarsh-Rose* model.
- These models were driven by the need of reducing the complexity of the Hodgkin-Huxley model, which would essentially still replicate the dynamics.
- Catherine Morris and Harold Lecar[4] proposed a two-dimensional "reduced" conductance-based description of the neuron dynamics.
- This model now has two state variables, namely the membrane potential (V) and the recovery variable (N), which is the conductance probability of Potassium channel.

[4] Morris, C. and Lecar, H. "Voltage oscillations in the barnacle giant muscle fiber". Biophys. J., 35, 193 (1981).

A brief survey of computational neuron dynamics models

- Since then, a notable number of neurodynamics models have been proposed.
- Popular ones include the *FitzHugh-Nagumo* model, the *Morris-Lecar* model, and the *Hindmarsh-Rose* model.
- These models were driven by the need of reducing the complexity of the Hodgkin-Huxley model, which would essentially still replicate the dynamics.
- Catherine Morris and Harold Lecar[4] proposed a two-dimensional "reduced" conductance-based description of the neuron dynamics.
- This model now has two state variables, namely the membrane potential (V) and the recovery variable (N), which is the conductance probability of Potassium channel.
- This model exhibits both Class I and II excitability.

[4] Morris, C. and Lecar, H. "Voltage oscillations in the barnacle giant muscle fiber". Biophys. J., 35, 193 (1981).

A denatured Morris-Lecar neuron model

- A simplified variant of the Morris-Lecar neuron was introduced in their book by Schaeffer and Cain, which has been dubbed as the *denatured* Morris-Lecar (dML) model.

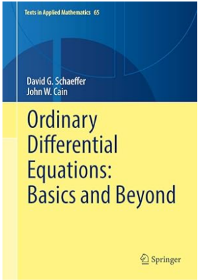

Figure: Book by Scheffer and Cain[5].

[5] D. Schaeffer and J. Cain, "Ordinary differential equations: Basics and beyond". (Springer, 2018).

A denatured Morris-Lecar neuron model

- The model equations are

$$
\begin{aligned}
\dot{x} &= x^2(1 - x) - y + I, \\
\dot{y} &= Ae^{\alpha x} - \gamma y.
\end{aligned}
$$

A denatured Morris-Lecar neuron model

- The model equations are
$$\dot{x} = x^2(1 - x) - y + I,$$
$$\dot{y} = Ae^{\alpha x} - \gamma y.$$
- These models are computationally efficient compared to the conductance-based models.

A denatured Morris-Lecar neuron model

- The model equations are
$$\dot{x} = x^2(1-x) - y + I,$$
$$\dot{y} = Ae^{\alpha x} - \gamma y.$$
- These models are computationally efficient compared to the conductance-based models.
- Here, x is the voltage-like variable with a cubic nonlinearity, and y represents the corresponding recovery variable.

A denatured Morris-Lecar neuron model

- The model equations are
$$\dot{x} = x^2(1-x) - y + I,$$
$$\dot{y} = Ae^{\alpha x} - \gamma y.$$
- These models are computationally efficient compared to the conductance-based models.
- Here, x is the voltage-like variable with a cubic nonlinearity, and y represents the corresponding recovery variable.
- The nonlinear term in x demonstrates positive feedback to neurons corresponding to self-reinforcement, leading to neuron firing.

A denatured Morris-Lecar neuron model

- The model equations are
$$\dot{x} = x^2(1-x) - y + I,$$
$$\dot{y} = Ae^{\alpha x} - \gamma y.$$
- These models are computationally efficient compared to the conductance-based models.
- Here, x is the voltage-like variable with a cubic nonlinearity, and y represents the corresponding recovery variable.
- The nonlinear term in x demonstrates positive feedback to neurons corresponding to self-reinforcement, leading to neuron firing.
- The exponential term in y models a negative feedback, corresponding to the dynamics of the refractory period.

A denatured Morris-Lecar neuron model

- External stimulus current I can be both positive and negative.

A denatured Morris-Lecar neuron model

- External stimulus current I can be both positive and negative.
- Other parameters A, α, and γ are all positive constants.

A denatured Morris-Lecar neuron model

- External stimulus current I can be both positive and negative.
- Other parameters A, α, and γ are all positive constants.
- Parameter γ is the excitability and together with A determines the kinetics of y.

A denatured Morris-Lecar neuron model

- External stimulus current I can be both positive and negative.
- Other parameters A, α, and γ are all positive constants.
- Parameter γ is the excitability and together with A determines the kinetics of y.
- Whereas α is a control parameter influencing the exponential growth rate of y.

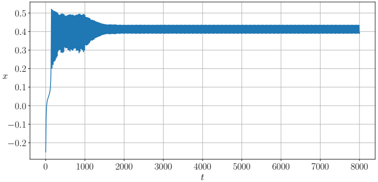

(a) Time series

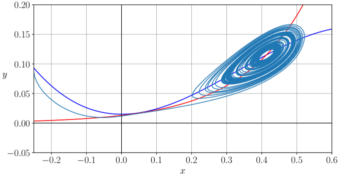

(b) Phase portrait

A denatured Morris-Lecar neuron model

- The dML model is closely comparable to a FitzHugh-Nagumo type neuron model which can be written as

$$\dot{x} = x^2(1 - x) - y + I,$$
$$\dot{y} = Ax - \gamma y.$$

A denatured Morris-Lecar neuron model

- The dML model is closely comparable to a FitzHugh-Nagumo type neuron model which can be written as

$$\dot{x} = x^2(1-x) - y + I,$$
$$\dot{y} = Ax - \gamma y.$$

- Both models have the same x-nullclines with differing y-nullclines. The y-nullclines curve upward pertaining to the exponential growth term $Ae^{\alpha x}$, whereas for FHN the y-nullclines are straight lines pertaining to the linear term Ax.

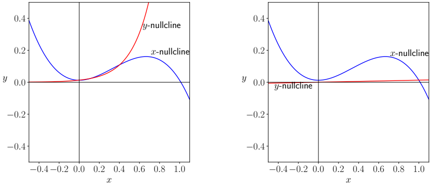

(a) dML (b) FHN

Figure: For parameter values $A = 0.0041$, $\alpha = 5.276$, $\gamma = 0.315$, and $I = 0.012347$.

Qualitative analysis

- The equilibrium can be computed from the transcendental equations[6]

$$x^2(1-x) - y + I = 0,$$
$$Ae^{\alpha x} - \gamma y = 0,$$

by solving for x.

[6] I. Ghosh, H.O. Fatoyinbo. "Fractional order induced bifurcations in Caputo-type denatured Morris-Lecar neurons". arXiv preprint arXiv:2502.17798 (2025).

Qualitative analysis

- The equilibrium can be computed from the transcendental equations[6]

$$x^2(1-x) - y + I = 0,$$
$$Ae^{\alpha x} - \gamma y = 0,$$

  by solving for x.
- We can write I as a function of x, y:

$$I_\infty(x) = \frac{A}{\gamma} e^{\alpha x} - x^2(1-x).$$

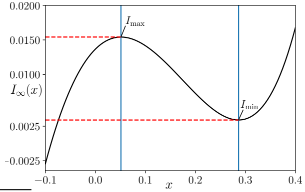

[6] I. Ghosh, H.O. Fatoyinbo. "Fractional order induced bifurcations in Caputo-type denatured Morris-Lecar neurons". arXiv preprint arXiv:2502.17798 (2025).

Qualitative analysis

- $I_\infty(x)$ is C^k smooth,

Qualitative analysis

- $I_\infty(x)$ is C^k smooth,
- $\lim_{x\to-\infty} I_\infty(x) = -\infty$, $\lim_{x\to\infty} I_\infty(x) = \infty$, and

Qualitative analysis

- $I_\infty(x)$ is C^k smooth,
- $\lim_{x\to-\infty} I_\infty(x) = -\infty$, $\lim_{x\to\infty} I_\infty(x) = \infty$, and
- $I_\infty(x)$ has two extrema, one maximum at $x_{\max}$ and one minimum at $x_{\min}$.

Qualitative analysis

- $I_\infty(x)$ is C^k smooth,
- $\lim_{x\to-\infty} I_\infty(x) = -\infty$, $\lim_{x\to\infty} I_\infty(x) = \infty$, and
- $I_\infty(x)$ has two extrema, one maximum at $x_{\max}$ and one minimum at $x_{\min}$.
- Let us consider $I_{\max} = I_\infty(x_{\max})$ and $I_{\min} = I_\infty(x_{\min})$.

Qualitative analysis

- $I_\infty(x)$ is C^k smooth,
- $\lim_{x\to-\infty} I_\infty(x) = -\infty$, $\lim_{x\to\infty} I_\infty(x) = \infty$, and
- $I_\infty(x)$ has two extrema, one maximum at $x_{\max}$ and one minimum at $x_{\min}$.
- Let us consider $I_{\max} = I_\infty(x_{\max})$ and $I_{\min} = I_\infty(x_{\min})$.
- if $I < I_{\min}$ or $I > I_{\max}$, the dML will have a unique equilibrium point (See (a), (b)),

Qualitative analysis

- $I_\infty(x)$ is C^k smooth,
- $\lim_{x\to-\infty} I_\infty(x) = -\infty$, $\lim_{x\to\infty} I_\infty(x) = \infty$, and
- $I_\infty(x)$ has two extrema, one maximum at $x_{\max}$ and one minimum at $x_{\min}$.
- Let us consider $I_{\max} = I_\infty(x_{\max})$ and $I_{\min} = I_\infty(x_{\min})$.
- if $I < I_{\min}$ or $I > I_{\max}$, the dML will have a unique equilibrium point (See (a), (b)),
- if $I = I_{\min}$ or $I = I_{\max}$, the dML will have two equilibrium points (See (c), (d)),

Qualitative analysis

- $I_\infty(x)$ is C^k smooth,
- $\lim_{x\to-\infty} I_\infty(x) = -\infty$, $\lim_{x\to\infty} I_\infty(x) = \infty$, and
- $I_\infty(x)$ has two extrema, one maximum at $x_{\max}$ and one minimum at $x_{\min}$.
- Let us consider $I_{\max} = I_\infty(x_{\max})$ and $I_{\min} = I_\infty(x_{\min})$.
- if $I < I_{\min}$ or $I > I_{\max}$, the dML will have a unique equilibrium point (See (a), (b)),
- if $I = I_{\min}$ or $I = I_{\max}$, the dML will have two equilibrium points (See (c), (d)),
- if $I \in (I_{\min}, I_{\max})$, it has three equilibrium points (See (e)).

Qualitative analysis

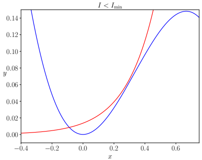

(a)

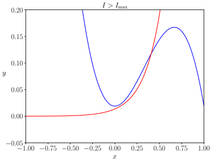

(b)

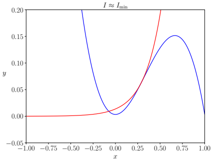

(c)

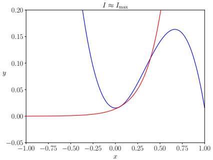

(d)

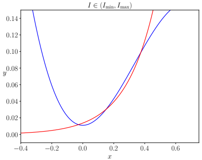

(e)

Qualitative analysis

- The Jacobian matrix for the dML at an equilibrium point (x^*, y^*) is

$$J = \begin{bmatrix} x^*(2-3x^*) & -1 \\ \alpha A e^{\alpha x^*} & -\gamma \end{bmatrix}.$$

Qualitative analysis

- The Jacobian matrix for the dML at an equilibrium point (x^*, y^*) is

$$J = \begin{bmatrix} x^*(2-3x^*) & -1 \\ \alpha A e^{\alpha x^*} & -\gamma \end{bmatrix}.$$

- Its trace and determinant are respectively given by

$$\begin{aligned} \tau(x^*) &= x^*(2-3x^*) - \gamma, \\ \delta(x^*) &= -\gamma x^*(2-3x^*) + \alpha A e^{\alpha x^*}. \end{aligned}$$

Qualitative analysis

- The Jacobian matrix for the dML at an equilibrium point (x^*, y^*) is

$$J = \begin{bmatrix} x^*(2-3x^*) & -1 \\ \alpha A e^{\alpha x^*} & -\gamma \end{bmatrix}.$$

- Its trace and determinant are respectively given by

$$\begin{aligned} \tau(x^*) &= x^*(2-3x^*) - \gamma, \\ \delta(x^*) &= -\gamma x^*(2-3x^*) + \alpha A e^{\alpha x^*}. \end{aligned}$$

- A *saddle-node* bifurcation occurs when $\delta(x^*) = 0$.

Qualitative analysis

- The Jacobian matrix for the dML at an equilibrium point (x^*, y^*) is

$$J = \begin{bmatrix} x^*(2-3x^*) & -1 \\ \alpha A e^{\alpha x^*} & -\gamma \end{bmatrix}.$$

- Its trace and determinant are respectively given by

$$\tau(x^*) = x^*(2-3x^*) - \gamma,$$
$$\delta(x^*) = -\gamma x^*(2-3x^*) + \alpha A e^{\alpha x^*}.$$

- A *saddle-node* bifurcation occurs when $\delta(x^*) = 0$.
- A *Hopf* bifurcation occurs when $\tau(x^*) = 0$ and $\delta(x^*) > 0$.

Qualitative analysis

- The Jacobian matrix for the dML at an equilibrium point (x^*, y^*) is

$$J = \begin{bmatrix} x^*(2-3x^*) & -1 \\ \alpha A e^{\alpha x^*} & -\gamma \end{bmatrix}.$$

- Its trace and determinant are respectively given by

$$\begin{aligned} \tau(x^*) &= x^*(2-3x^*) - \gamma, \\ \delta(x^*) &= -\gamma x^*(2-3x^*) + \alpha A e^{\alpha x^*}. \end{aligned}$$

- A *saddle-node* bifurcation occurs when $\delta(x^*) = 0$.
- A *Hopf* bifurcation occurs when $\tau(x^*) = 0$ and $\delta(x^*) > 0$.
- These codimension-one bifurcation computations require hand calculations and might not always be analytically tractable.

Numerical Bifurcation Analysis

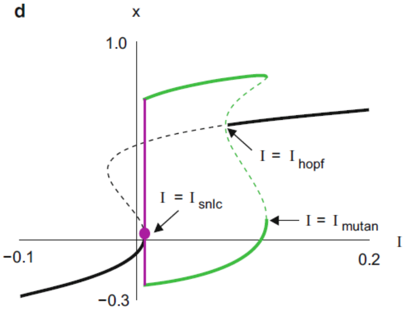

Figure: (a) SNLC: Saddle Node Limit Cycle, (b) I_{mutan}: a mutual annihilation bifurcation occurs at $I = I_{\mathrm{mutan}}$. See D. Schaeffer and J. Cain,(Springer, 2018).

Numerical Bifurcation Analysis

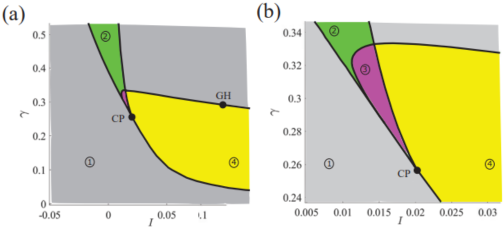

Figure: A codimension-two bifurcation diagram of the dML model in the (I, γ)-plane[7].

[7]H.O. Fatoyinbo, *et al.* "Numerical bifurcation analysis of improved denatured morris-lecar neuron model". In 2022 international conference on decision aid sciences and applications (DASA) (pp. 55-60). IEEE (2022).

Effect of Electromagnetic Flux

- The dML model is perturbed where the membrane potential x is subjected to an electromagnetic flux term ϕ.

[7] Source: `https://www.mayoclinic.org/tests-procedures/deep-brain-stimulation/about/pac-20384562`

Effect of Electromagnetic Flux

- The dML model is perturbed where the membrane potential x is subjected to an electromagnetic flux term ϕ.
- This technique makes the model more physically realistic by implementing complex dynamics.

[7] Source: `https://www.mayoclinic.org/tests-procedures/deep-brain-stimulation/about/pac-20384562`

Effect of Electromagnetic Flux

- The dML model is perturbed where the membrane potential x is subjected to an electromagnetic flux term ϕ.
- This technique makes the model more physically realistic by implementing complex dynamics.
- This has practical applications and relevance in scenarios like *deep brain simulation* (DBS), and calls for an extensive mathematical modeling.

[7] Source: `https://www.mayoclinic.org/tests-procedures/deep-brain-stimulation/about/pac-20384562`

Effect of Electromagnetic Flux

- The dML model is perturbed where the membrane potential x is subjected to an electromagnetic flux term ϕ.
- This technique makes the model more physically realistic by implementing complex dynamics.
- This has practical applications and relevance in scenarios like *deep brain simulation* (DBS), and calls for an extensive mathematical modeling.
- DBS involves putting an electrode deep inside the brain and treating people with mobility conditions.

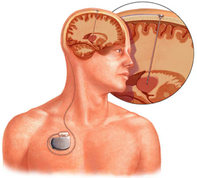

[7] Source: `https://www.mayoclinic.org/tests-procedures/deep-brain-stimulation/about/pac-20384562`

Effect of Electromagnetic Flux

- The model is improved to a three-dimensional version with $\phi(t)$ as the new dynamical variable

$$\begin{aligned}
\dot{x} &= x^2(1-x) - y + I + k\rho(\phi)x, \\
\dot{y} &= Ax - \gamma y, \\
\dot{\phi} &= k_1 x - k_2 \phi + \phi_{\text{ext}}.
\end{aligned}$$

Effect of Electromagnetic Flux

- The model is improved to a three-dimensional version with $\phi(t)$ as the new dynamical variable

$$\begin{aligned}\dot{x} &= x^2(1-x) - y + I + k\rho(\phi)x,\\ \dot{y} &= Ax - \gamma y,\\ \dot{\phi} &= k_1 x - k_2\phi + \phi_{\text{ext}}.\end{aligned}$$

- Here k is the feedback gain,

Effect of Electromagnetic Flux

- The model is improved to a three-dimensional version with $\phi(t)$ as the new dynamical variable

$$
\begin{aligned}
\dot{x} &= x^2(1-x) - y + I + k\rho(\phi)x, \\
\dot{y} &= Ax - \gamma y, \\
\dot{\phi} &= k_1 x - k_2 \phi + \phi_{\text{ext}}.
\end{aligned}
$$

- Here k is the feedback gain,
- function $\rho(\phi) = \alpha + 2\beta\phi^2$ is the electromagnetic effect on the action potential,

Effect of Electromagnetic Flux

- The model is improved to a three-dimensional version with $\phi(t)$ as the new dynamical variable

$$\begin{aligned}\dot{x} &= x^2(1-x) - y + I + k\rho(\phi)x,\\ \dot{y} &= Ax - \gamma y,\\ \dot{\phi} &= k_1 x - k_2\phi + \phi_{\text{ext}}.\end{aligned}$$

- Here k is the feedback gain,
- function $\rho(\phi) = \alpha + 2\beta\phi^2$ is the electromagnetic effect on the action potential,
- ϕ is the magnetic flux across the cell membrane,

Effect of Electromagnetic Flux

- The model is improved to a three-dimensional version with $\phi(t)$ as the new dynamical variable

$$\dot{x} = x^2(1-x) - y + I + k\rho(\phi)x,$$
$$\dot{y} = Ax - \gamma y,$$
$$\dot{\phi} = k_1 x - k_2\phi + \phi_{\text{ext}}.$$

- Here k is the feedback gain,
- function $\rho(\phi) = \alpha + 2\beta\phi^2$ is the electromagnetic effect on the action potential,
- ϕ is the magnetic flux across the cell membrane,
- parameter α and β are the memory conductances, and

Effect of Electromagnetic Flux

- The model is improved to a three-dimensional version with $\phi(t)$ as the new dynamical variable

$$\begin{aligned}\dot{x} &= x^2(1-x) - y + I + k\rho(\phi)x,\\ \dot{y} &= Ax - \gamma y,\\ \dot{\phi} &= k_1 x - k_2\phi + \phi_{\text{ext}}.\end{aligned}$$

- Here k is the feedback gain,
- function $\rho(\phi) = \alpha + 2\beta\phi^2$ is the electromagnetic effect on the action potential,
- ϕ is the magnetic flux across the cell membrane,
- parameter α and β are the memory conductances, and
- ϕ_{ext} is the external magnetic flux.

Effect of Electromagnetic Flux

- The model is improved to a three-dimensional version with $\phi(t)$ as the new dynamical variable

$$\begin{aligned}
\dot{x} &= x^2(1-x) - y + I + k\rho(\phi)x, \\
\dot{y} &= Ax - \gamma y, \\
\dot{\phi} &= k_1 x - k_2\phi + \phi_{\text{ext}}.
\end{aligned}$$

- Here k is the feedback gain,
- function $\rho(\phi) = \alpha + 2\beta\phi^2$ is the electromagnetic effect on the action potential,
- ϕ is the magnetic flux across the cell membrane,
- parameter α and β are the memory conductances, and
- ϕ_{ext} is the external magnetic flux.
- The external current can be modeled as a periodic function $I = I_0 \sin(\omega t)$, with I_0 as the current amplitude and ω is the angular frequency.

Effect of Electromagnetic Flux

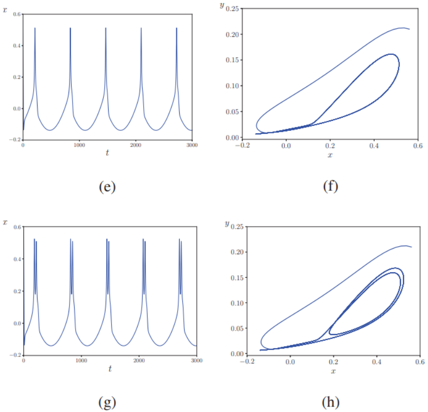

Figure: Time series and Phase portrait with increasing I_0

Effect of Electromagnetic Flux

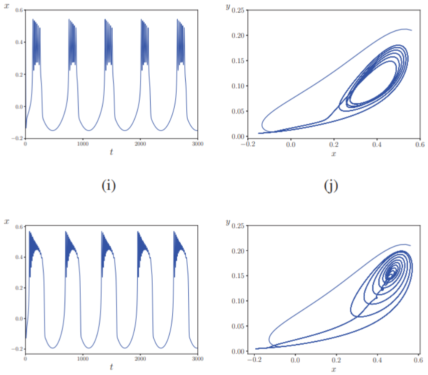

Figure: Time series and Phase portrait with increasing I_0

- The external periodic current produces multiple-mode bursting activities.

A slow-fast variant

- The slow-fast version of the dML also introduced by Schaeffer and Cain is given by

$$\dot{x} = x^2(1-x) - y + I,$$
$$\dot{y} = Ae^{\alpha x} - \gamma y,$$
$$\dot{I} = \varepsilon(I'(x) - I),$$

A slow-fast variant

- The slow-fast version of the dML also introduced by Schaeffer and Cain is given by

$$\begin{aligned}\dot{x} &= x^2(1-x) - y + I,\\ \dot{y} &= Ae^{\alpha x} - \gamma y,\\ \dot{I} &= \varepsilon(I'(x) - I),\end{aligned}$$

- where

$$I'(x) = \frac{1}{60}\left[1 + \tanh\left(\frac{0.05 - x}{0.001}\right)\right]$$

is the smoothed-out version of a step function.

A slow-fast variant

- The slow-fast version of the dML also introduced by Schaeffer and Cain is given by

$$\begin{aligned}
\dot{x} &= x^2(1-x) - y + I,\\
\dot{y} &= Ae^{\alpha x} - \gamma y,\\
\dot{I} &= \varepsilon(I'(x) - I),
\end{aligned}$$

- where

$$I'(x) = \frac{1}{60}\left[1 + \tanh\left(\frac{0.05 - x}{0.001}\right)\right]$$

  is the smoothed-out version of a step function.
- the parameter ε is a small perturbation parameter that separates the time scales and is sometimes referred to as the *time-scale parameter*.

A slow-fast variant

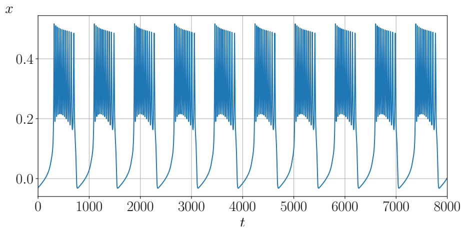

(a) Time series

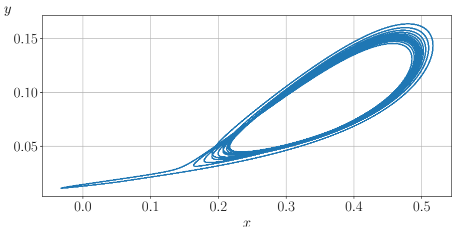

(b) Phase portrait

Figure: We observe a periodic bursting behavior. Here $A = 0.0041$, $\alpha = 5.276$, $\gamma = 0.315$, and $\varepsilon = 0.001$. The initial condition $x(0)$ is sampled uniformly from the range $[-1, 1]$. Furthermore $(y(0), I(0)) = (0.1, 0.012347)$.

A slow-fast variant

- Neurons manifest repeated rapid bursting with quiet intervals.

[8] E. Izhikevich, "Dynamical systems in neuroscience". (MIT press, 2007).

A slow-fast variant

- Neurons manifest repeated rapid bursting with quiet intervals.
- For a certain range of the current I, Shaeffer and Cain argued that the dynamics would consist of both a stable periodic solution and a stable equilibrium point.

[8] E. Izhikevich, "Dynamical systems in neuroscience". (MIT press, 2007).

A slow-fast variant

- Neurons manifest repeated rapid bursting with quiet intervals.
- For a certain range of the current I, Shaeffer and Cain argued that the dynamics would consist of both a stable periodic solution and a stable equilibrium point.
- This bistability ultimately leads to bursting.

[8] E. Izhikevich, "Dynamical systems in neuroscience". (MIT press, 2007).

A slow-fast variant

- Neurons manifest repeated rapid bursting with quiet intervals.
- For a certain range of the current I, Shaeffer and Cain argued that the dynamics would consist of both a stable periodic solution and a stable equilibrium point.
- This bistability ultimately leads to bursting.
- This would be possible if I were allowed to vary slowly in time.

[8] E. Izhikevich, "Dynamical systems in neuroscience". (MIT press, 2007).

A slow-fast variant

- Neurons manifest repeated rapid bursting with quiet intervals.
- For a certain range of the current I, Shaeffer and Cain argued that the dynamics would consist of both a stable periodic solution and a stable equilibrium point.
- This bistability ultimately leads to bursting.
- This would be possible if I were allowed to vary slowly in time.
- This kind of bursting is classified as *fold/homoclinic* type[8] where the transition from the resting state to the spiking limit cycle occurs via a saddle-node (fold) bifurcation and from the spiking state to the resting state via a saddle homoclinic orbit bifurcation.

[8] E. Izhikevich, "Dynamical systems in neuroscience". (MIT press, 2007).

Fold/homoclinic burster

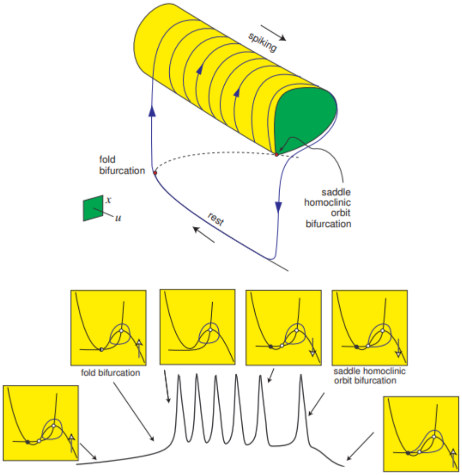

Figure 9.25: "Fold/homoclinic" bursting. The resting state disappears via saddle-node (fold) bifurcation, and the spiking limit cycle disappears via saddle homoclinic orbit bifurcation.

Qualitative analysis

- To compute X^*, the first step requires solving the nonlinear transcendental equation given by,

$$x^{*2}\left(1-x^*\right)-\frac{A}{\gamma}e^{\alpha x^*}+I'(x^*)=0,$$

which is analytically intractable and can only be solved using a numerical solver.

- The Jacobian of the system (1) is given by

$$J=\begin{bmatrix} x(2-3x) & -1 & 1 \\ \alpha A e^{\alpha x} & -\gamma & 0 \\ \mathcal{L}(x) & 0 & -\varepsilon \end{bmatrix}.$$

Qualitative analysis

- Here

$$\tau(x) = x(2-3x) - \gamma - \varepsilon$$

is the trace of J,

$$\sigma(x) = \gamma\varepsilon - (\gamma+\varepsilon)x(2-3x) + \alpha A e^{\alpha x} - \mathcal{L}(x)$$

is the second trace of J, and

$$\delta(x) = x(2-3x)\gamma\varepsilon - \varepsilon\alpha A e^{\alpha x} + \gamma\mathcal{L}(x)$$

is the determinant of J.

Qualitative analysis

- Here

$$\tau(x) = x(2-3x) - \gamma - \varepsilon$$

is the trace of J,

$$\sigma(x) = \gamma\varepsilon - (\gamma+\varepsilon)x(2-3x) + \alpha A e^{\alpha x} - \mathcal{L}(x)$$

is the second trace of J, and

$$\delta(x) = x(2-3x)\gamma\varepsilon - \varepsilon\alpha A e^{\alpha x} + \gamma\mathcal{L}(x)$$

is the determinant of J.

- Note that

$$\mathcal{L}(x) = -\frac{50\varepsilon}{3}\operatorname{sech}^2\left[50\left(1-20x\right)\right].$$

Qualitative analysis

- Here

$$\tau(x) = x(2-3x) - \gamma - \varepsilon$$

is the trace of J,

$$\sigma(x) = \gamma\varepsilon - (\gamma+\varepsilon)x(2-3x) + \alpha A e^{\alpha x} - \mathcal{L}(x)$$

is the second trace of J, and

$$\delta(x) = x(2-3x)\gamma\varepsilon - \varepsilon\alpha A e^{\alpha x} + \gamma\mathcal{L}(x)$$

is the determinant of J.

- Note that

$$\mathcal{L}(x) = -\frac{50\varepsilon}{3}\mathrm{sech}^2\left[50\left(1-20x\right)\right].$$

- The eigenvalues μ_i, $i = 1, \ldots, 3$ can be evaluated from J at the equilibrium point by solving the third order characteristic equation $P_3(\mu) = 0$

Codimension-one bifurcation diagram

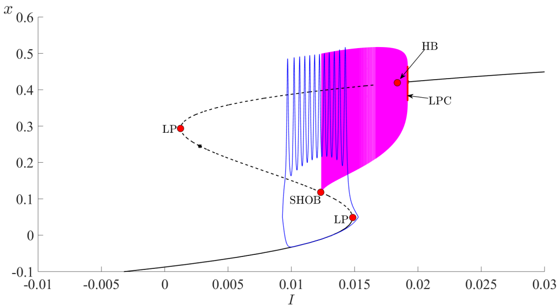

Figure: Codimension-one bifurcation diagram of the fast subsystem with superimposition of the periodic bursting of the slow-fast system. Solid [dashed] curves correspond to stable [unstable] solutions and magenta curves are limit cycles. HB, LP, SHOB, and LPC represent Hopf bifurcation, saddle-node bifurcation of an equilibrium, saddle-homoclinic orbit bifurcation and saddle-node bifurcation of cycles respectively. Here $A = 0.0041$, $\alpha = 5.276$, $\gamma = 0.315$, and $\varepsilon = 0.001$ with the initial condition as $(x(0), y(0), I(0)) = (0.5, 0.1, 0.012347)$.

Neuron Synapse

- Neurons communicate with each other through *synapses*.

[9] Source: `https://qbi.uq.edu.au/brain-basics/brain/brain-physiology/action-potentials-and-synapses`

Neuron Synapse

- Neurons communicate with each other through *synapses*.
- Synapses convert an electrical signal propagated by a neuron into a chemical signal in the form of neurotransmitter release.

[9] Source: `https://qbi.uq.edu.au/brain-basics/brain/brain-physiology/action-potentials-and-synapses`

Neuron Synapse

- Neurons communicate with each other through *synapses*.
- Synapses convert an electrical signal propagated by a neuron into a chemical signal in the form of neurotransmitter release.
- The neurotransmitter can either excite or inhibit the second neuron from firing its own action potential[9].

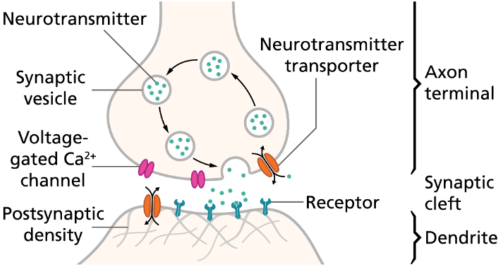

[9]Source: `https://qbi.uq.edu.au/brain-basics/brain/brain-physiology/action-potentials-and-synapses`

Two-coupled dML neurons

- Two connected neurons can be mathematically modeled using a directional coupling strategy.

[10] I. Ghosh, H.O. Fatoyinbo, and S.S. Muni. "Comprehensive analysis of slow-fast denatured Morris-Lecar neurons". Phys. Rev. E 111.4 (2025): 044204.

Two-coupled dML neurons

- Two connected neurons can be mathematically modeled using a directional coupling strategy.
- In our work[10] a linear coupling replicating a bidirectional electrical synapse is utilized. The neurons are considered identical.

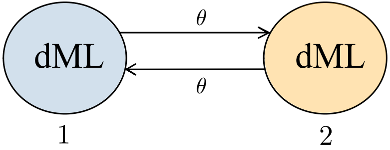

[10] I. Ghosh, H.O. Fatoyinbo, and S.S. Muni. "Comprehensive analysis of slow-fast denatured Morris-Lecar neurons". Phys. Rev. E 111.4 (2025): 044204.

Two-coupled dML neurons

- Two connected neurons can be mathematically modeled using a directional coupling strategy.
- In our work[10] a linear coupling replicating a bidirectional electrical synapse is utilized. The neurons are considered identical.

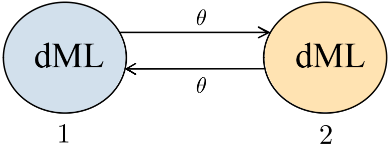

- The model equations are

$$\dot{x}_1 = x_1^2(1 - x_1) - y_1 + I_1 + \theta(x_2 - x_1), \quad \dot{y}_1 = Ae^{\alpha x_1} - \gamma y_1, \quad \dot{I}_1 = \varepsilon(I'(x_1) - I_1),$$
$$\dot{x}_2 = x_2^2(1 - x_2) - y_2 + I_2 + \theta(x_1 - x_2), \quad \dot{y}_2 = Ae^{\alpha x_2} - \gamma y_2, \quad \dot{I}_2 = \varepsilon(I'(x_2) - I_2).$$

[10] I. Ghosh, H.O. Fatoyinbo, and S.S. Muni. "Comprehensive analysis of slow-fast denatured Morris-Lecar neurons". Phys. Rev. E 111.4 (2025): 044204.

Time series & phase portraits

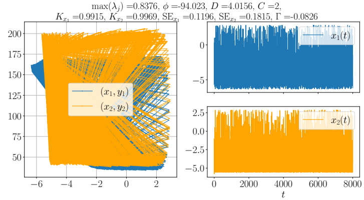

(a) $\theta = -15$, $\varepsilon = 0.0002$: Hyperchaotic

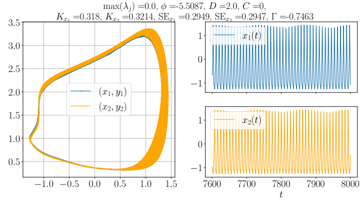

(b) $\theta = -1$, $\varepsilon = 0.0002$: Quasiperiodic

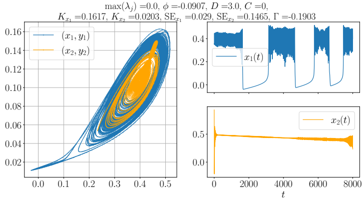

(c) $\theta = 0$, $\varepsilon = 0.0002$: irregular bursting

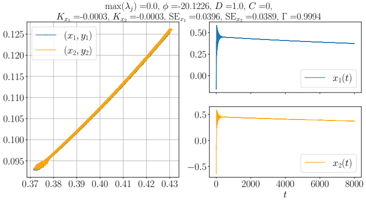

(d) $\theta = 10$, $\varepsilon = 0.0002$: Decay oscillations

Time series & phase portraits

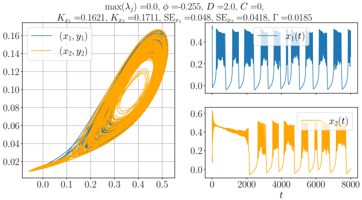

(e) $\theta = 0$, $\varepsilon = 0.001$: Mixed mode

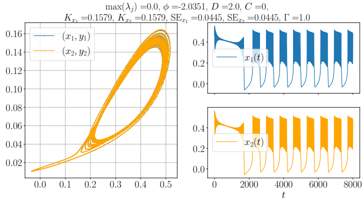

(f) $\theta = 1$, $\varepsilon = 0.001$: Mixed mode

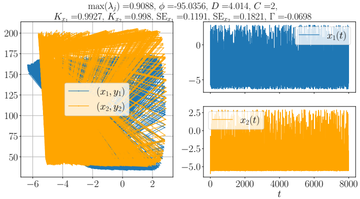

(g) $\theta = -15$, $\varepsilon = 0.1$: Hyperchaotic

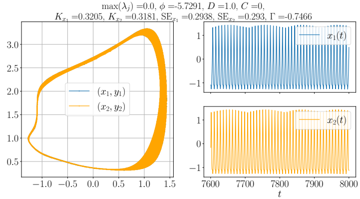

(h) $\theta = -1$, $\varepsilon = 0.1$: Quasiperiodic

Codimension-one bifurcation diagram

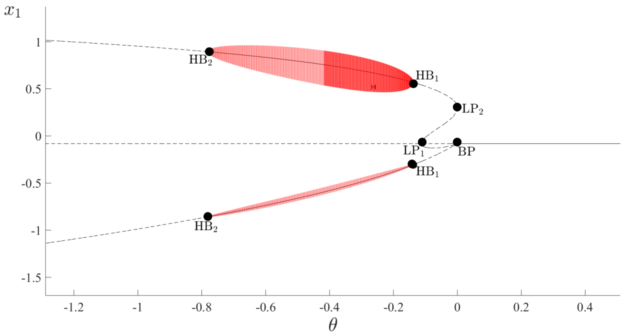

Figure: Codimension-one bifurcation diagram of the coupled fast subsystem. Solid [dashed] curves correspond to stable [unstable] solutions and red curves are limit cycles. HB, LP, and BP represent Hopf bifurcation, saddle-node bifurcation of an equilibrium and branch point respectively.

The $0 - 1$ test for detecting chaos

- The $0 - 1$ test[11] is applied to the time series data of x_1, x_2 generated from the simulation.

[11] G. Gottwald and I. Melbourne, On the implementation of the 0–1 test for chaos, SIAM J. Appl. Dyn. Syst. 8, 129 (2009).

The $0 - 1$ test for detecting chaos

- The $0 - 1$ test[11] is applied to the time series data of x_1, x_2 generated from the simulation.
- For a time series data denoted by $\{x(n), n = 1, \ldots, M\}$, the first step in the $0 - 1$ test is the computation of the two translation variables p_e and q_e (with $e \in (0, 2\pi)$)

$$p_e(n) = \sum_{k=1}^{n} x(k)\cos(ek),$$
$$q_e(n) = \sum_{k=1}^{n} x(k)\sin(ek),$$

[11] G. Gottwald and I. Melbourne, On the implementation of the 0–1 test for chaos, SIAM J. Appl. Dyn. Syst. 8, 129 (2009).

The $0-1$ test for detecting chaos

- The $0-1$ test[11] is applied to the time series data of x_1, x_2 generated from the simulation.
- For a time series data denoted by $\{x(n), n = 1, \ldots, M\}$, the first step in the $0-1$ test is the computation of the two translation variables p_e and q_e (with $e \in (0, 2\pi)$)

$$p_e(n) = \sum_{k=1}^{n} x(k)\cos(ek),$$
$$q_e(n) = \sum_{k=1}^{n} x(k)\sin(ek),$$

- The p_e vs. q_e plot will typically be bounded for regular dynamics or will approximately behave like a two-dimensional diffusive Brownian motion with evolution rate $\sqrt{n}$ and zero drift for chaos.

[11] G. Gottwald and I. Melbourne, On the implementation of the 0–1 test for chaos, SIAM J. Appl. Dyn. Syst. 8, 129 (2009).

The $0-1$ test for detecting chaos

- This can be inferred from the mean square displacement, given by

$$m_e(n) = \frac{1}{M}\sum_{i=1}^{M}\left[\{p_e(i+n)-p_e(i)\}^2 + \{q_e(i+n)-q_e(i)\}^2\right].$$

The $0 - 1$ test for detecting chaos

- This can be inferred from the mean square displacement, given by

$$m_e(n) = \frac{1}{M} \sum_{i=1}^{M} \left[\{p_e(i+n) - p_e(i)\}^2 + \{q_e(i+n) - q_e(i)\}^2 \right].$$

- The asymptotic growth rate is given by

$$k_e = \lim_{n \to \infty} \frac{\log m_e(n)}{\log n}.$$

The $0-1$ test for detecting chaos

- This can be inferred from the mean square displacement, given by

$$m_e(n) = \frac{1}{M}\sum_{i=1}^{M}\left[\{p_e(i+n)-p_e(i)\}^2 + \{q_e(i+n)-q_e(i)\}^2\right].$$

- The asymptotic growth rate is given by

$$k_e = \lim_{n\to\infty}\frac{\log m_e(n)}{\log n}.$$

- $k_e \sim 1$ indicates chaos and $k_e \sim 0$ indicates regularity.

The $0-1$ test for detecting chaos

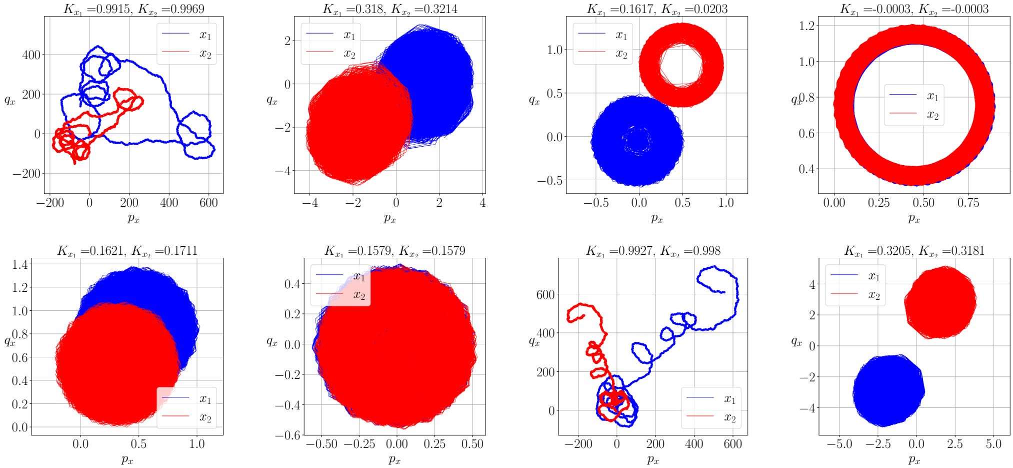

Sample entropy: for measuring complexity

- The *sample entropy* quantifies the complexity of the time series.

[12] J. Richman and J. Moorman, Physiological time- series analysis using approximate entropy and sample entropy, Am. J. Physiol. Heart Circ. Physiol. 278 (2000).

Sample entropy: for measuring complexity

- The *sample entropy* quantifies the complexity of the time series.
- This is built on the algorithm put forward by Richman and Moorman[12].

[12] J. Richman and J. Moorman, Physiological time- series analysis using approximate entropy and sample entropy, Am. J. Physiol. Heart Circ. Physiol. 278 (2000).

Sample entropy: for measuring complexity

- The *sample entropy* quantifies the complexity of the time series.
- This is built on the algorithm put forward by Richman and Moorman[12].
- A higher sample entropy implies higher complexity

[12] J. Richman and J. Moorman, Physiological time- series analysis using approximate entropy and sample entropy, Am. J. Physiol. Heart Circ. Physiol. 278 (2000).

Cross-correlation coefficient for synchronization

- We can quantify the collective behaviour of the dimer.

Cross-correlation coefficient for synchronization

- We can quantify the collective behaviour of the dimer.
- This is advocated by the synchronization measure.

Cross-correlation coefficient for synchronization

- We can quantify the collective behaviour of the dimer.
- This is advocated by the synchronization measure.
- Pearson's correlation coefficient can be adopted to come up with the *cross-correlation coefficient*.

Cross-correlation coefficient for synchronization

- We can quantify the collective behaviour of the dimer.
- This is advocated by the synchronization measure.
- Pearson's correlation coefficient can be adopted to come up with the *cross-correlation coefficient*.
- The cross-correlation coefficient between node 1 and 2 given by

$$\Gamma = \frac{\langle \tilde{x}_1(t)\tilde{x}_2(t)\rangle}{\sqrt{\langle \tilde{x}_1(t)^2\rangle\langle \tilde{x}_2(t)^2\rangle}},$$

Cross-correlation coefficient for synchronization

- We can quantify the collective behaviour of the dimer.
- This is advocated by the synchronization measure.
- Pearson's correlation coefficient can be adopted to come up with the *cross-correlation coefficient*.
- The cross-correlation coefficient between node 1 and 2 given by

$$\Gamma = \frac{\langle \tilde{x}_1(t)\tilde{x}_2(t)\rangle}{\sqrt{\langle \tilde{x}_1(t)^2\rangle\langle \tilde{x}_2(t)^2\rangle}},$$

- where $\tilde{x}_i(t) = x_i(t) - \langle x_i(t)\rangle$ is the variation of the dynamical variable x at index i from its mean.

Cross-correlation coefficient for synchronization

- We can quantify the collective behaviour of the dimer.
- This is advocated by the synchronization measure.
- Pearson's correlation coefficient can be adopted to come up with the *cross-correlation coefficient*.
- The cross-correlation coefficient between node 1 and 2 given by

$$\Gamma = \frac{\langle \tilde{x}_1(t)\tilde{x}_2(t)\rangle}{\sqrt{\langle \tilde{x}_1(t)^2\rangle\langle \tilde{x}_2(t)^2\rangle}},$$

- where $\tilde{x}_i(t) = x_i(t) - \langle x_i(t)\rangle$ is the variation of the dynamical variable x at index i from its mean.
- The angular brackets $\langle\cdot\rangle$ signify the mean over time.

Cross-correlation coefficient for synchronization

- We can quantify the collective behaviour of the dimer.
- This is advocated by the synchronization measure.
- Pearson's correlation coefficient can be adopted to come up with the *cross-correlation coefficient*.
- The cross-correlation coefficient between node 1 and 2 given by

$$\Gamma = \frac{\langle \tilde{x}_1(t)\tilde{x}_2(t)\rangle}{\sqrt{\langle \tilde{x}_1(t)^2\rangle\langle \tilde{x}_2(t)^2\rangle}},$$

- where $\tilde{x}_i(t) = x_i(t) - \langle x_i(t)\rangle$ is the variation of the dynamical variable x at index i from its mean.
- The angular brackets $\langle\cdot\rangle$ signify the mean over time.
- When $|\Gamma| = 1$, it means both the nodes are completely synchronized with each other.

Cross-correlation coefficient for synchronization

- We can quantify the collective behaviour of the dimer.
- This is advocated by the synchronization measure.
- Pearson's correlation coefficient can be adopted to come up with the *cross-correlation coefficient*.
- The cross-correlation coefficient between node 1 and 2 given by

$$\Gamma = \frac{\langle \tilde{x}_1(t)\tilde{x}_2(t)\rangle}{\sqrt{\langle \tilde{x}_1(t)^2\rangle\langle \tilde{x}_2(t)^2\rangle}},$$

- where $\tilde{x}_i(t) = x_i(t) - \langle x_i(t)\rangle$ is the variation of the dynamical variable x at index i from its mean.
- The angular brackets $\langle\cdot\rangle$ signify the mean over time.
- When $|\Gamma| = 1$, it means both the nodes are completely synchronized with each other.
- When $\Gamma = 1$ it means both the nodes are in phase and completely synchronized, whereas $\Gamma = -1$ represents anti-phase synchrony.

Numerics

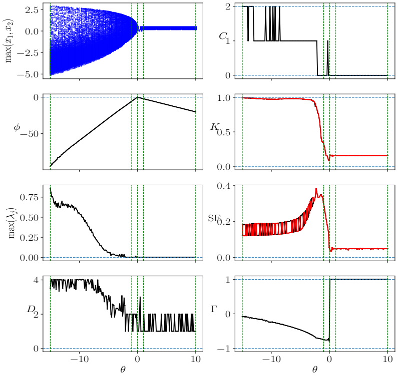

(a) $\varepsilon = 0.001$

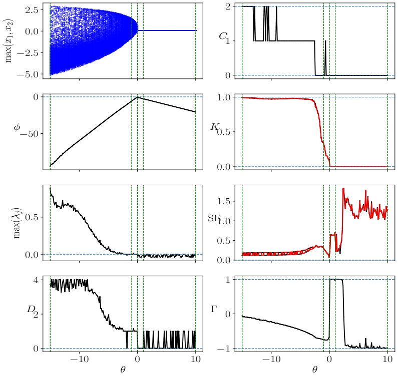

(b) $\varepsilon = 0.1$

Fractional order version

- Now we model the dML neuron as a set of *Caputo-type* fractional order differential equations. Fractional-order systems incorporate memory effects.

[13] B. Lundstrom, M. Higgs, W. Spain, A. Fairhall. "Fractional differentiation by neocortical pyramidal neurons". Nat. Neurosci. 11, 1335–1342 (2008).

[14] T. Anastasio. "The fractional-order dynamics of brainstem vestibulo-oculomotor neurons". Biol. Cyber. 72, 69–79 (1994).

Fractional order version

- Now we model the dML neuron as a set of *Caputo-type* fractional order differential equations. Fractional-order systems incorporate memory effects.
- Lundstrom *et al.*[13] argued that there exists a multiple time scale adaptation in single rat neocortical neurons which is consistent with fractional order differential equations.

[13]B. Lundstrom, M. Higgs, W. Spain, A. Fairhall. "Fractional differentiation by neocortical pyramidal neurons". Nat. Neurosci. 11, 1335–1342 (2008).

[14]T. Anastasio. "The fractional-order dynamics of brainstem vestibulo-oculomotor neurons". Biol. Cyber. 72, 69–79 (1994).

Fractional order version

- Now we model the dML neuron as a set of *Caputo-type* fractional order differential equations. Fractional-order systems incorporate memory effects.
- Lundstrom *et al.*[13] argued that there exists a multiple time scale adaptation in single rat neocortical neurons which is consistent with fractional order differential equations.
- Anastasio[14] suggested that the oculomotor integrator in the brain that controls eye movements, might be fractional-order.

---

[13] B. Lundstrom, M. Higgs, W. Spain, A. Fairhall. "Fractional differentiation by neocortical pyramidal neurons". Nat. Neurosci. 11, 1335–1342 (2008).

[14] T. Anastasio. "The fractional-order dynamics of brainstem vestibulo-oculomotor neurons". Biol. Cyber. 72, 69–79 (1994).

Fractional order version

- Now we model the dML neuron as a set of *Caputo-type* fractional order differential equations. Fractional-order systems incorporate memory effects.
- Lundstrom *et al.*[13] argued that there exists a multiple time scale adaptation in single rat neocortical neurons which is consistent with fractional order differential equations.
- Anastasio[14] suggested that the oculomotor integrator in the brain that controls eye movements, might be fractional-order.
- The model equations are

$$
\begin{aligned}
{}^{C}\mathcal{D}_0^{\beta} x &= x^2(1-x) - y + I, \\
{}^{C}\mathcal{D}_0^{\beta} y &= Ae^{\alpha x} - \gamma y.
\end{aligned}
$$

[13] B. Lundstrom, M. Higgs, W. Spain, A. Fairhall. "Fractional differentiation by neocortical pyramidal neurons". Nat. Neurosci. 11, 1335–1342 (2008).

[14] T. Anastasio. "The fractional-order dynamics of brainstem vestibulo-oculomotor neurons". Biol. Cyber. 72, 69–79 (1994).

Fractional order version

- Now we model the dML neuron as a set of *Caputo-type* fractional order differential equations. Fractional-order systems incorporate memory effects.
- Lundstrom *et al.*[13] argued that there exists a multiple time scale adaptation in single rat neocortical neurons which is consistent with fractional order differential equations.
- Anastasio[14] suggested that the oculomotor integrator in the brain that controls eye movements, might be fractional-order.
- The model equations are

$$
\begin{aligned}
{}^{C}\mathcal{D}_0^{\beta} x &= x^2(1-x) - y + I, \\
{}^{C}\mathcal{D}_0^{\beta} y &= Ae^{\alpha x} - \gamma y.
\end{aligned}
$$

- Here C stands for "Caputo" and $\beta \in (0, 1]$ is the order of the integral, also known as the *memory index*.

[13] B. Lundstrom, M. Higgs, W. Spain, A. Fairhall. "Fractional differentiation by neocortical pyramidal neurons". Nat. Neurosci. 11, 1335–1342 (2008).

[14] T. Anastasio. "The fractional-order dynamics of brainstem vestibulo-oculomotor neurons". Biol. Cyber. 72, 69–79 (1994).

Qualitative analysis

Theorem

Suppose

i) $x^*(2-3x^*)-\gamma>0$, *and*
ii) $-\gamma x^*(2-3x^*)+\alpha A e^{\alpha x^*}<2\sqrt{-\gamma-x^*(2-3x^*)}\cos(\frac{\beta\pi}{2})$.

Then an equilibrium point (x^*,y^*) of the fractional order system is asymptotically stable.

Theorem

Suppose $I\in(I_{\min},I_{\max})$. Then this branch of equilibrium points is completely unstable.

- From the above theorem we can directly see that $\delta(x^*)<0$ implies one of the two eigenvalues is positive and the other negative, meaning the equilibrium point on this branch is a saddle, irrespective of the fractional order $\beta\in(0,1]$.

Theorem

Suppose $I=I_{\min}$ or $I=I_{\max}$. Then the fractional order system has a saddle-node *bifurcation.*

Qualitative analysis

Theorem

Suppose $I < I_{\min}$ or $I > I_{\max}$. Then

i) *the stability of an equilibrium point of the system depends on the sign of $\tau(x^*)$,*

ii) *for $\tau(x^*) \geq 0$ the equilibrium is asymptotically stable if and only if the order*

$$\beta < \beta^* = \frac{2}{\pi} \cos^{-1} \left(\min \left(1, \frac{-\gamma + x^*(2 - 3x^*)}{2\sqrt{\alpha A e^{\alpha x^*} - \gamma x^*(2 - 3x^*)}} \right) \right).$$

Phase portraits

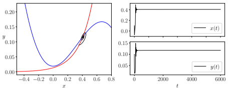

(a) $\beta = 0.9$

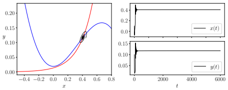

(b) $\beta = 0.92$

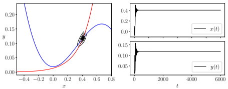

(c) $\beta = 0.94$

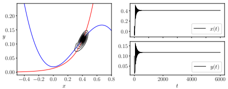

(d) $\beta = 0.96$

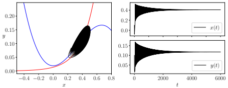

(e) $\beta = 0.98$

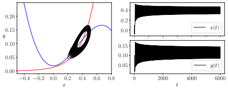

(f) $\beta = \beta^*$

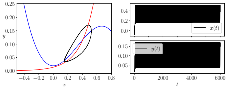

(g) $\beta = 0.99$

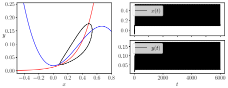

(h) $\beta = 1$

A crude bifurcation diagram

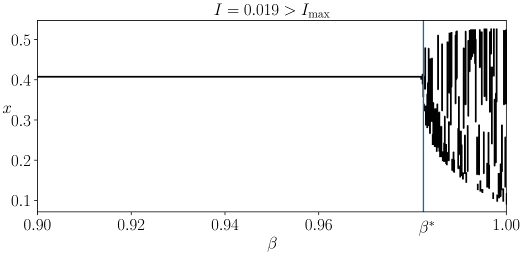

(a) $\beta^* \approx 0.98233$

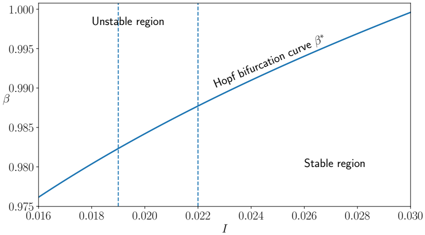

(b) Hopf bifurcation curve

Discussion/Future work

- We aim to consider a higher-order network of the neurons (more realistic)

Discussion/Future work

- We aim to consider a higher-order network of the neurons (more realistic)
- We also aim to study pattern formation in a diffusively coupled chain of neurons

Discussion/Future work

- We aim to consider a higher-order network of the neurons (more realistic)
- We also aim to study pattern formation in a diffusively coupled chain of neurons
- Delay-induced coupling is an interesting avenue to explore.

Discussion/Future work

- We aim to consider a higher-order network of the neurons (more realistic)
- We also aim to study pattern formation in a diffusively coupled chain of neurons
- Delay-induced coupling is an interesting avenue to explore.
- An adaptive coupling strategy based on the Hebbian learning rule is justifiable.

Discussion/Future work

- We aim to consider a higher-order network of the neurons (more realistic)
- We also aim to study pattern formation in a diffusively coupled chain of neurons
- Delay-induced coupling is an interesting avenue to explore.
- An adaptive coupling strategy based on the Hebbian learning rule is justifiable.
- It would be intriguing to investigate the dynamical behaviour of the coupled neurons as a game-theoretic model.

The End

Thank you! Questions?